*Desalination and Water Treatment*
www.deswater.com
doi: 10.5004/dwt.2023.29510

292 (2023) 131–140
April

# Adsorption of Cd(II) and Pb(II) by Mg-modified straw biochar

Jianfeng Li

*School of Civil Engineering, Architecture and Environment, Hubei University of Technology, Wuhan 430068, China, email: 101910672@hbut.edu.cn*

Received 23 October 2022; Accepted 27 March 2023

**ABSTRACT**

In this work, magnesium-modified rice straw biochar (MgBC) was prepared by chemical impregnation, and the effects of proportion, initial pH, contact time, temperature and initial concentration on the removal of Cd(II) and Pb(II) by MgBC were investigated. Additionally, scanning electron microscopy, Brunauer–Emmett–Teller, Fourier-transform infrared spectroscopy (FTIR) and X-ray diffraction (XRD) were used for the characterisation of MgBC. The results shown that MgBC surface contained massive Mg-particles and possessed more abundant O-containing groups. Batch adsorption experiments shown that the optimum adsorption efficiency of Cd(II) and Pb(II) by MgBC was achieved at ratio of 1:2 and initial pH of 6.0. The pseudo-second-order kinetic model and the Langmuir isothermal model could better describe the removal of Cd(II) and Pb(II) by MgBC. The maximum adsorption capacity of Cd(II) and Pb(II) by MgBC was 92.68 and 128.06 mg/g at pH 6.0, 35°C and initial concentrations of 10~100 mg/L, respectively. FTIR and XRD analysis shown that the removal mechanism of Cd(II) and Pb(II) by MgBC involved complexation, ions exchange, co-precipitation and electrostatic interaction. After 4 adsorption–desorption experiment, the removal efficiency of Cd(II) and Pb(II) by MgBC remained above 80%. This results indicated that MgBC had great potential for the treatment of wastewater containing Cd(II) and Pb(II).

*Keywords:* Mg-modification; Straw biochar; Cd(II); Pb(II); Adsorption mechanism

## 1. Introduction

With the rapid development of agriculture and industry, heavy metal pollution become a serious environmental pollution problem, and pose a serious threat to human health. Heavy metals are nondegradable by microorganisms and can accumulate through bioconcentration, which are extremely harmful to human, animal and plant [1,2]. Cadmium Cd(II) and lead Pb(II), as one of the most representative and hazardous heavy metal, are mainly discharged from electroplating, metal mining drainage, textile printing and dyeing industries [3–5]. The research of the containment and effective treatment of Cd(II) and Pb(II) wastewater is of great environmental importance. The main treatment methods for Cd(II) and Pb(II) containing wastewater include precipitation, ion exchange, membrane filtration and adsorption [6–8]. Adsorption is considered to be one of the most researched and environmentally friendly method [9,10].

Biochar is a carbon rich material produced by the biomass pyrolysis under oxygen-limited condition [11,12]. Compared with other carbon materials, biochar possesses the advantages of wide sources of raw materials, simple preparation methods and low prices [9,13]. Furthermore, biochar has received increasing attention in the fields of greenhouse gas emission mitigation, soil fertilization and environmental remediation [14–16]. Nevertheless, the performance of biochar obtained by direct pyrolysis of biomass to remove contaminants is limited, which may be related to the limited active adsorption sites of original biochar [3,17]. To enhance the adsorption performance of virgin biochar, various methods have been used to modify biochar, including acid/alkali modification, organic solvent modification, and metal salt/

oxide modification [18–21]. Among these modification methods, biochar prepared with metal salt/oxide as modifier is currently the material with better adsorption performance, with Mn, Mg and Fe being the commonest used salt/oxides modifier [1,6,17,22]. Cao et al. [22] demonstrated that the adsorption capacity of Cd(II) and Pb(II) on iron sulphide decorated biochar was 57.71 and 124.62 mg/g, respectively. Nevertheless, the MnOx-impregnated peanut shell biochar adsorbed 36.77 and 164.59 mg/g of Cd(II) and Pb(II), respectively [17]. Mg-modified biochar provides more adsorption sites and demonstrates better adsorption performance in the pollutants adsorption [23,24]. However, MgO possesses the disadvantage of high surface energy, easy agglomeration and small size, which limits its adsorption performance on contaminants [25]. The uniform dispersion of Mg particles on biochar matrix is an effective way to improve the stability of Mg particles [26]. Notably, the effectiveness of Mg-containing biochar for the removal of pollutants (e.g., lead, arsenic, phosphate and chromium) has been investigated [12,16,24,26,27]. The adsorption capacity of the MgO-loaded porous biochar reach 1625.5 mg/g for Pb(II) [28]. Additionally, previous literature shown that the adsorption capacity of phosphate by MgO-biochar was 111.20 mg/g [24]. Furthermore, the adsorption capacities of the MgO-loaded rice husk biochar and the corn cob biochar were 21.32 and 16.31 mg/g for ammonia nitrogen, respectively [12]. Therefore, Mg-modified biochar was chosen as the adsorbent in this study to investigate the adsorption performance of heavy metal ions. According to our literature survey, there are no studies in the literature on the preparation of Mg-modified biochar from rice straw biochar impregnated with $MgCl_2$ solution and used for the removal of Cd(II) and Pb(II) from aqueous solution.

In this work, Mg-modified biochar composites (MgBC) were prepared by chemical impregnation method. The adsorption performance of MgBC on Cd(II) and Pb(II) was investigated. Moreover, the removal mechanism of MgBC on Cd(II) and Pb(II) was analyzed. This work proposes to provide an effective adsorbent material for the remediation of Cd(II) and Pb(II) containing wastewater.

## 2. Materials and methods

### 2.1. Reagents

Reagents: magnesium chloride $MgCl_2$, cadmium nitrate $Cd(NO_3)_2$, lead nitrate $Pb(NO_3)_2$ and hydrochloric acid HCl were analytically reagent (AR) and were purchased from Sinopharm Reagent Group (Shanghai, China). Different mass concentrations of Cd(II) and Pb(II) were prepared by certain mass of $Cd(NO_3)_2$ and $Pb(NO_3)_2$, respectively. Rice straw was collected from a farmland in Wuhan, China.

### 2.2. Preparation of materials

Rice straw biochar: rice straw was crushed to 1~10 cm, and then dried to constant weight in constant temperature oven at 80°C. 5 g dried rice straw was placed on a porcelain boat and placed in a muffle furnace. $N_2$ was iintroduced into the muffle as a protective gas and the muffle was then heated up to 400°C at rate of 10°C/min. After 2 h of pyrolysis, the black solid was collected from the boat and washed several times with 1 mol/L HCl. The black solid was dried and recorded as BC.

Mg-modified rice straw biochar (MgBC): a certain proportion of $MgCl_2$ and BC was added to 100 mL of deionized water and sonicated for 120 min. The mixed solution was placed in a water bath at 80°C and 150 r/min to react 120 min. After the reaction was completed, the solution was filtered. The collected solids were washed several times with deionised water and dried under vacuum for 12 h to obtain Mg-modified rice straw biochar composite.

### 2.3. Batch adsorption experiments

0.4 g/L MgBC and 10 mL metal ion solution were added to 25 mL conical flask, which was placed in constant temperature oscillator at 25°C and 150 rpm to study the effects of ratio (4:1~1:4), initial pH (2.0~8.0), reaction time (5~300 min), temperature (15°C, 25°C and 35°C) and initial concentration (10~100 mg/L) on the removal of Pb(II) and Cd(II). The solution was filtered after the adsorption equilibrium, and the filtrate was collected to determine the remaining concentration of Pb(II) and Cd(II) by flame atomic absorption spectrophotometry (Shimadzu, Model AA-6300, Japan), and to calculate the removal efficiency [Eq. (1)] and the adsorption capacity [Eq. (2)].

$$R = \frac{C_0 - C_e}{C_0} \times 100\% \tag{1}$$

$$q = \frac{\left(C_0 - C_e\right)V}{m} \tag{2}$$

where $R$ is the removal efficiency, %; $C_0$ is the initial concentration, mg/L; $C_e$ is the remaining concentration in solution after adsorption equilibrium, mg/L; $q$ is the adsorption capacity, mg/g; $V$ is the solution volume, mL; $m$ is the adsorbent mass, mg.

### 2.4. Adsorption–desorption experiment

After adsorption of 10 mg/L of Pb(II) and Cd(II) solution, the solution was centrifuged for 10 min and then filtered. The reacted MgBC was desorbed by shaking in 0.01 mol/L HCl for 6 h. Afterwards, the desorbed MgBC was dried in oven at 80°C for 2 h. The procedure was repeated 8 times and the Pb(II) and Cd(II) removal efficiencies were calculated after each adsorption–desorption experiment. Moreover, the concentration of $Mg^{2+}$ in the desorbed and adsorbed solution was determined by flame atomic absorption spectrophotometry.

## 3. Results and discussion

### 3.1. Characterization analysis

The specific surface area, pore volume and average pore size (Table 1) of MgBC were lower than those of BC, presumably due to the Mg particles loading. The microstructures of BC and MgBC were analysed by scanning electron

microscopy (SEM). As shown in Fig. 1a and b, there were some grooves and pore structures on the surface of BC. However, the surface of MgBC (Fig. 1c and d) showed a lot of granular material and a reduction in pore structure. The reduction in pore structure observed on the MgBC surface was also consistent with the pore parameters analysis.

The surface functional groups of BC and MgBC were analyzed by Fourier-transform infrared spectroscopy (FTIR) and the results are shown in Fig. 2a. The main functional groups of BC were –OH (3,435 $cm^{-1}$), C=O/C=C (1,621 $cm^{-1}$) and C–O (1,078 $cm^{-1}$). This result indicated that BC held abundance of O-containing functional groups. In the FTIR spectrum of MgBC, the wavenumber of –OH group was shifted to 3,339 $cm^{-1}$ and the intensity of –OH was enhanced, indicating that the Mg-modification was able to increase the content of –OH groups in the biochar. Additionally, the peaks at 1,617 $cm^{-1}$ (C=O/C=C) and 1,081 $cm^{-1}$, (C–O) also changed after modification. Notably, the Si–O group shown an enhancement of the vibrational peak after modification, indicating the successful introduction of the Mg–O group [20].

Table 1
Pore structure analysis of BC and MgBC

| | Specific surface area ($m^2/g$) | Pore volume ($cm^3/g$) | Pore size (nm) |
|---|---|---|---|
| BC | 114.78 | 0.254 | 5.75 |
| MgBC | 82.39 | 0.108 | 4.79 |

The crystalline structures of BC and MgBC were analysed using X-ray diffraction (XRD), as shown in Fig. 2b. The diffraction peaks at 2θ = 23.34° and 42.66° were considered to be the C peaks in the BC. However, the C peaks in MgBC appeared to weaken or disappear. Additionally, the diffraction

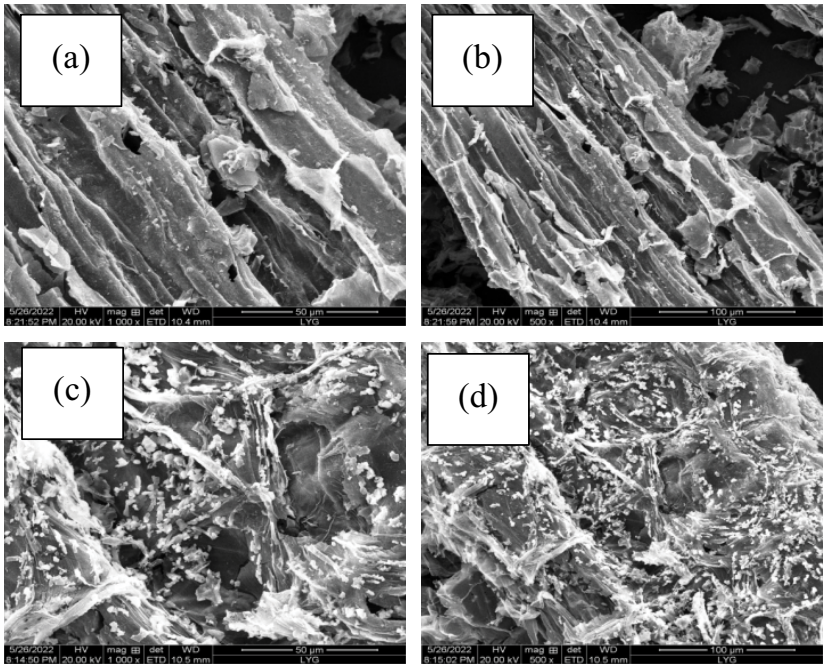


Fig. 1. Scanning electron microscopy images of BC (a, b) and MgBC (c, d).

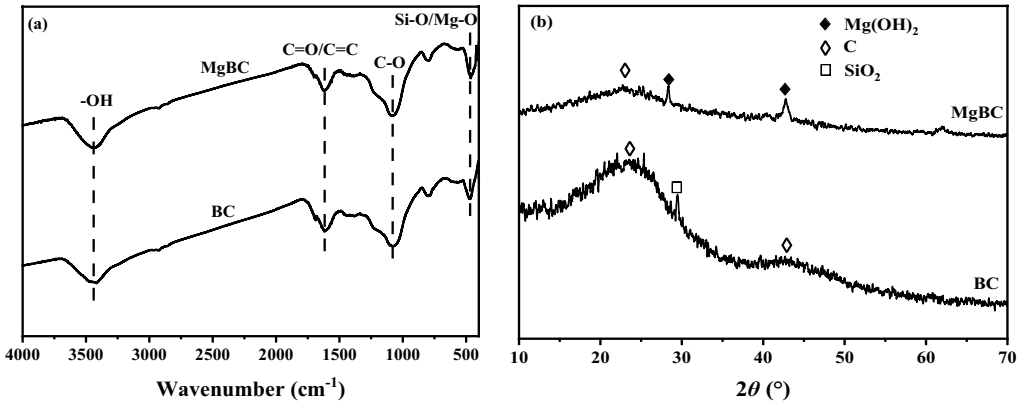


Fig. 2. Fourier-transform infrared spectroscopy (a) and X-ray diffraction (b) patterns of BC and MgBC.

peak of $SiO_2$ at 2θ = 29.40° also disappeared after the modification [29]. Notably, two new diffraction peaks appear at 2θ = 28.28° and 42.72°, which were $Mg(OH)_2$ and proved the successful preparation of the MgBC composite [19].

### *3.2. Effect of reaction conditions on the removal of Cd(II) and Pb(II) by MgBC*

#### *3.2.1. Material ratio*

The effect of proportioning on the removal of Cd(II) and Pb(II) was investigated. The removal efficiency increased gradually with increasing ratio, and the maximum removal efficiency of Cd(II) and Pb(II) was 93.64% and 96.78% at the ratio of 1:2, respectively. However, with the ratio greater than 1:2, the removal efficiency of Cd(II) and Pb(II) decreased to 88.65% and 90.38%, respectively, presumably because the excess MgO covered the surface of BC causing agglomeration and thus reducing the specific surface area [20]. The dissolved concentrations of $Mg^{2+}$ for different materials are shown in Fig. 3b. As the ratio of $MgCl_2$ decreased, the concentration of $Mg^{2+}$ in the solution gradually decreased. To reduce the leaching concentration of $Mg^{2+}$ and to ensure the removal efficiency, the subsequent experiment was carried out in a ratio of 1:2.

#### *3.2.2. Initial pH of the solution*

The effect of initial pH (2.0~8.0) on the removal of Cd(II) and Pb(II) by MgBC was investigated, as shown in Fig. 4. At pH 2.0, the removal efficiency of Cd(II) and Pb(II) by MgBC was 48.21% and 51.68%, respectively. At pH 6.0, the removal efficiency of Cd(II) and Pb(II) by MgBC reached 93.37% and 96.57%, respectively. As the initial pH of the solution increased to 8.0, a slight increase in the removal efficiency occurred. This was presumed to be that at lower pH values, a large number of $H^+$ ions occupied and protonated positively charged MgBC surface functional groups (e.g., hydroxyl and carboxyl groups), thus creating electrostatic repulsion with the positively charged Cd(II) and Pb(II), resulting in lower removal efficiency [7,30]. As the initial pH of the solution gradually increased above the $pH_{pzc}$ of MgBC (Fig. 4b, the $pH_{pzc}$ was 5.76), the functional groups deprotonated to become negatively charged and caused an increase in the removal efficiency [20,24]. Many studies shown that Cd(II) and Pb(II) hydrolysed to produce $Cd(OH)_2$ and $Pb(OH)_2$ precipitates, respectively [7,12]. When the initial pH was above 6.0, and the removal efficiency was increased. The above analysis suggested that the mechanism of Cd(II) and Pb(II) removal by MgBC may include electrostatic action and co-precipitation.

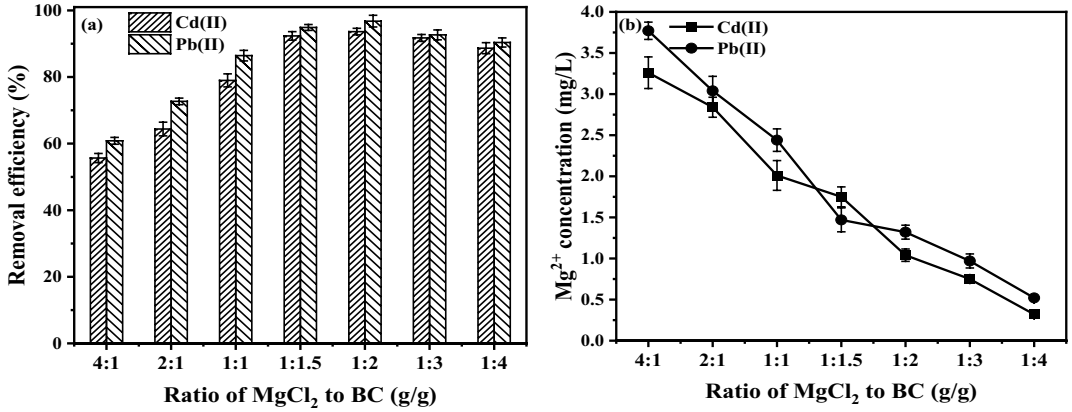


Fig. 3. Effect of the ratio on Cd(II) removal ($T$ = 25°C, dosage = 0.4 g/L, $C_0$ = 10 mg/L, and contact time = 300 min). The concentration of $Mg^{2+}$ in the adsorbed solution (b).

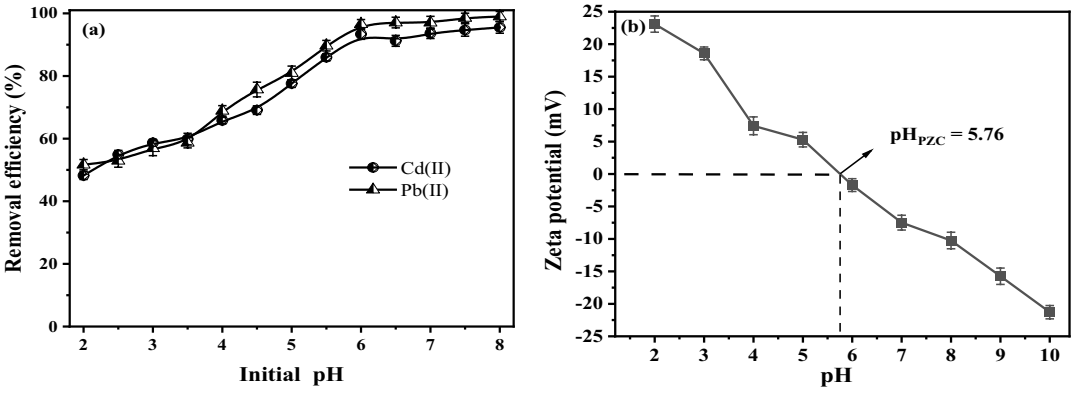


Fig. 4. Effect of the initial pH on the removal (a) and the zeta potential (b) analysis of MgBC ($T$ = 25°C, dosage = 0.4 g/L, $C_0$ = 10 mg/L, contact time = 300 min and ratio 1:2).

*3.2.3. Adsorption kinetics*

The effect of adsorption time (5~300 min) on the removal of Cd(II) and Pb(II) was investigated, as shown in Fig. 5. The adsorption of Cd(II) and Pb(II) by MgBC can basically be divided into three stages. During 5~60 min, the adsorption capacity of Cd(II) and Pb(II) by MgBC increased rapidly, which belonged to the fast adsorption stage. In the second slow adsorption phase, the adsorption capacity of MgBC on Pb(II) increased slowly from 60 to 150 min, and the adsorption capacity of MgBC on Cd(II) increased slowly from 60 to 180 min. The adsorption equilibrium was reached at 150 and 180 min for Cd(II) and Pb(II), respectively. The faster adsorption stage was due to the presence of a large number of unused adsorption sites on the surface of MgBC [4,6]. As the reaction time increased the number of available adsorption sites gradually decreased, resulting in a slow increase in adsorption to adsorption equilibrium [15,20]. To further understand the adsorption process of Cd(II) and Pb(II), the data were fitted using pseudo-first-order kinetic model [Eq. (3)] and pseudo-second-order kinetic model [Eq. (4)], and the results are shown in Fig. 5 and Table 2.

$$q_t = q_e\left(1 - e^{-k_1 t}\right) \tag{3}$$

$$q_t = \frac{q_e^2 k_2 t}{1 + q_e k_2 t} \tag{4}$$

where $q_e$ and $q_t$ are the adsorption volumes at adsorption equilibrium and time "$t$", respectively, mg/g; $k_1$ indicates the pseudo-first-order kinetic model adsorption rate constant, 1/min; $k_2$ is the pseudo-second-order kinetic model adsorption rate constant, g/(mg·min); and $t$ indicates the reaction time, min.

As shown in Table 3, the correlation coefficient of the pseudo-first-order kinetic model ($R^2$ = 0.6) was lower than that of the pseudo-second-order kinetic model ($R^2$ = 0.9), indicating that the adsorption processes of Cd(II) and Pb(II) were more consistent with the pseudo-second-order kinetic model, and also suggesting that the adsorption processes were chemical reaction (e.g., complexation, co-precipitation, and other chemical interactions) [2,11]. In Table 2, the actual equilibrium adsorption capacity of Cd(II) and Pb(II) was closer to the theoretical adsorption capacity of the pseudo-second-order kinetic model, which also indicated that the removal of Cd(II) and Pb(II) by MgBC was more consistent with the pseudo-second-order kinetic model [31,32]. Additionally, the adsorption rate constant for Pb(II) in the pseudo-second-order kinetic model was less than that for Cd(II), suggesting that the MgBC was able to adsorb Pb(II) faster and reach adsorption equilibrium more quickly [16,18]. This was presumed to be because the hydration radius of Pb(II) in aqueous solution was smaller than that of Cd(II). Therefore, MgBC had better affinity for Pb(II) adsorption and reached equilibrium more quickly.

*3.2.4. Adsorption isotherms*

The effect of concentration (10~100 mg/L) and temperature (15°C, 25°C and 35°C) was investigated. As the initial solution concentration increased, the adsorption capacity of Cd(II) and Pb(II) by MgBC first gradually increased and then tended to equilibrium, which was attributed to the

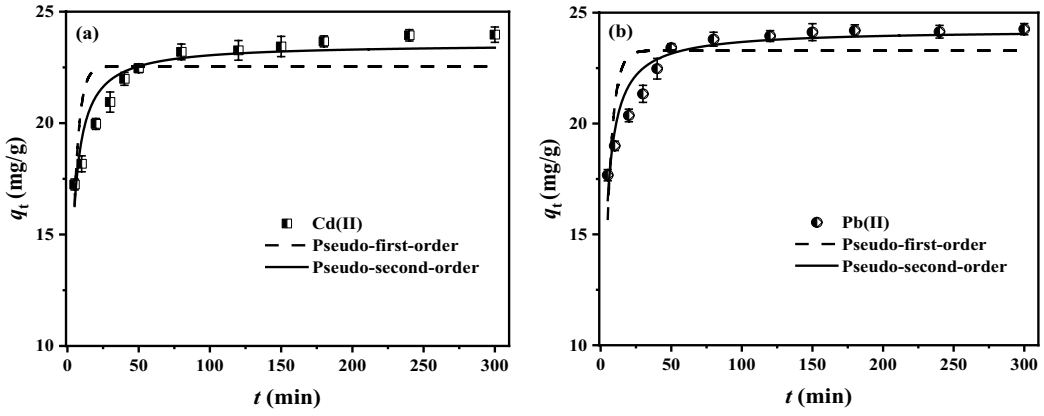


Fig. 5. Effect of adsorption time on removal and adsorption kinetics fitting curve ($T$ = 25°C, dosage = 0.4 g/L, $C_0$ = 10 mg/L, pH = 6.0 and material ratio 1:2).

Table 2
Kinetic fitting parameters

| | $q_{e,\exp}$ (mg/g) | Pseudo-first-order | | | Pseudo-second-order | | |
|---|---|---|---|---|---|---|---|
| | | $q_{e,\mathrm{cal}}$ (mg/g) | $k_1$ (min$^{-1}$) | $R^2$ | $q_e$ (mg/g) | $k_2$ (g/(mg·min)) | $R^2$ |
| Cd(II) | 23.97 | 22.54 | 0.258 | 0.637 | 23.56 | 0.019 | 0.907 |
| Pb(II) | 24.26 | 23.29 | 0.224 | 0.671 | 24.23 | 0.018 | 0.926 |

adsorption sites in MgBC were gradually all used as the concentration increased [24,33]. Moreover, the adsorption capacity of Cd(II) and Pb(II) by MgBC increased as the adsorption temperature increased, indicating that the adsorption process was heat absorption reaction [34]. The sorption data were fitted by the Langmuir model [Eq. (5)] and Freundlich model [Eq. (6)].

$$q_e = \frac{q_{\max} K_L C_e}{1 + K_L C_e} \tag{5}$$

$$q_e = K_f C_e^{1/n} \tag{6}$$

where $q_e$ is the adsorption amount at equilibrium, mg/g; $C_e$ is the concentration of metal ions at adsorption equilibrium, mg/L; $q_{\max}$ and $K_L$ are the maximum adsorption amount and the Langmuir equilibrium constant, respectively; $K_f$ and $n$ denote the Freundlich equilibrium constant and the dimensionless constant, respectively.

A comparison of the correlation coefficients ($R_1^2 > R_2^2$) indicated that the Langmuir model better fitted the removal of Cd(II) and Pb(II) by MgBC, reflecting the homogeneous, monolayer sorption [27,34]. Furthermore, the adsorption capacity increased gradually with increasing temperature, indicating that the adsorption of Cd(II) and Pb(II) by MgBC was heat-absorbing process and that increasing the adsorption temperature was beneficial to the adsorption [21,28]. The adsorption capacity of MgBC on Cd(II) and Pb(II) were 73.77 and 119.52 mg/g, respectively. In Table 4, the adsorption capacity of biochar for Cd(II) and Pb(II) with different modification methods was compared. The results demonstrated that the adsorption of Cd(II) and Pb(II) by MgBC was higher than that of surface-modified magnetic biochar [22], N/P enriched bamboo sawdust biochar [30], camellia seed husk biochar [19] and sulfide-iron decorated biochar [33], while the adsorption of Pb(II) by MgBC was only lower than that of MnOx-impregnated peanut shells derived biochar [17], indicating that Mg-modified biochar had the potential to remove Cd(II) and Pb(II) from aqueous solution.

### 3.3. Adsorption mechanism

To understand the adsorption mechanism, FTIR was used to characterize the functional groups of Cd/Pb loaded biochar (Fig. 7a). The interaction of MgBC with heavy metals resulted in a significant reduction and shift of the vibrational peak at 3,363 $cm^{-1}$ corresponding to the –OH, which was presumed to be the involvement of the hydroxyl group in the adsorption process [28,32]. The peaks of both the C=O and C–O groups of the carboxyl group (1,562 $cm^{-1}$) shown a decrease and shift, suggesting that C=O and C–O may be involved in the adsorption [1,22,34]. The changes in functional groups during the pre- and post-sorption process on biochar suggest that –OH, C=O and C–O may be involved in the adsorption of $Cd^{2+}$/$Pb^{2+}$ [3,20]. Notably, the Mg–O peak decreased after adsorption, presumably due to the ion exchange between Mg in MgBC and $Cd^{2+}$/$Pb^{2+}$ for the removal of heavy metals. This may be due to the ion exchange between Mg and Pb in MgBC [20,28,35]. Following adsorption, the characteristic XRD peaks for Pb(II) and Cd(II) were observed on MgBC, indicating the formation of Pb(II) and Cd(II) precipitates on the MgBC surface [4,20]. The characteristic peaks of the Pb(II) precipitates found from the XRD including $PbCO_3$, $Pb(OH)_2$ and $Pb_3(PO_4)_2$ [34,35]. For MgBC+Cd, the precipitates mainly

Table 3
Fitting parameters of adsorption isotherm

| | $T$ (°C) | Langmuir model | | | Freundlich model | | |
|---|---|---|---|---|---|---|---|
| | | $q_{\max}$ (mg/g) | $K_L$ (L/mg) | $R_1^2$ | $K_f$ ($mg^{1-n}\cdot L^n/g$) | $n$ | $R_2^2$ |
| Cd(II) | 15 | 64.94 | 0.894 | 0.974 | 28.53 | 4.47 | 0.818 |
| | 25 | 73.77 | 1.126 | 0.995 | 32.71 | 4.56 | 0.857 |
| | 35 | 92.68 | 0.994 | 0.987 | 37.01 | 3.81 | 0.798 |
| Pb(II) | 15 | 117.46 | 0.670 | 0.989 | 48.96 | 3.910 | 0.801 |
| | 25 | 119.52 | 1.423 | 0.969 | 58.91 | 4.689 | 0.795 |
| | 35 | 128.06 | 1.628 | 0.976 | 64.52 | 4.814 | 0.731 |

Table 4
Comparison of the Cd(II) and Pb(II) adsorption capacity of different biochar material

| | Method | Cd(II) (mg/g) | Pb(II) (mg/g) | References |
|---|---|---|---|---|
| Surface-modified magnetic biochar | Chemical reagents modification | 61.25 | 53.75 | [18] |
| N/P enriched bamboo sawdust biochar | Guanidine phosphate activation | 38.3 | 104.40 | [30] |
| Camellia seed husk biochar | HCl oxidation | 68.22 | 109.67 | [19] |
| Sulfide-iron decorated biochar | FeS modification | 57.71 | 124.62 | [22] |
| Peanut shells derived biochar | MnOx-impregnated | 36.77 | 164.59 | [17] |
| Mg-modification straw biochar | $MgCl_2$-impregnation | 92.68 | 128.06 | This work |

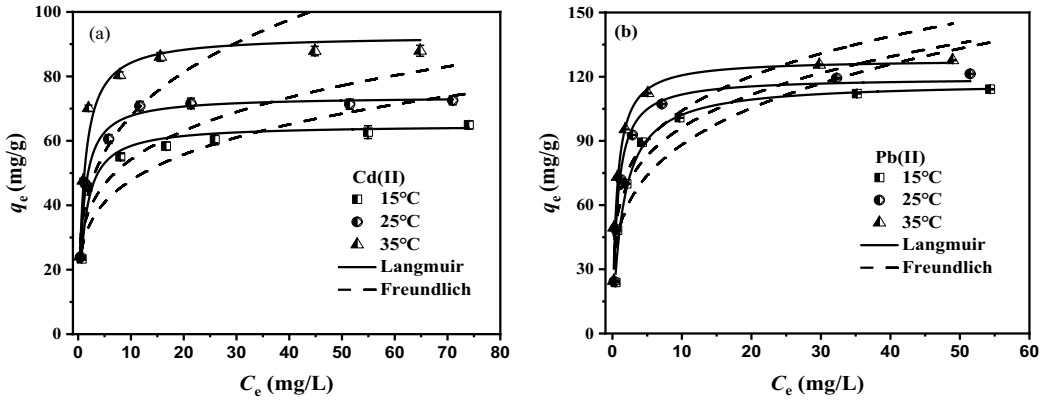


Fig. 6. Effect of temperature and initial concentration on removal and the adsorption isotherm fitting curve ($T$ = 25°C, dosage = 0.4 g/L, contact time = 300 min, pH = 6.0 and material ratio 1:2).

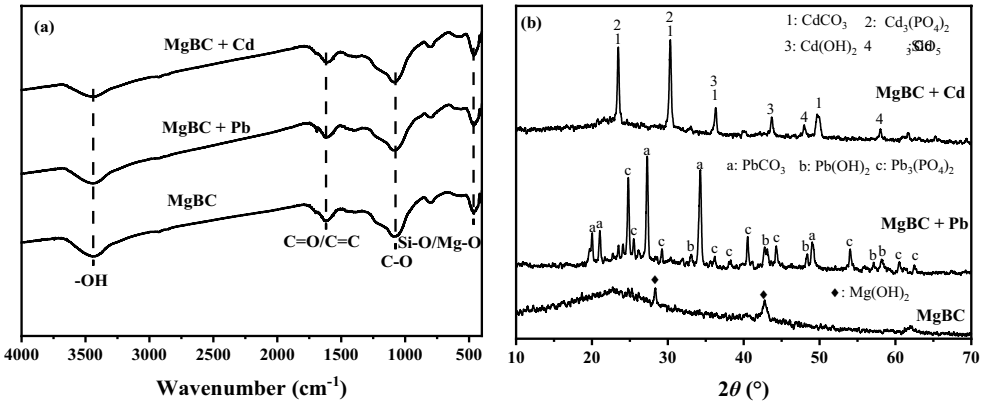


Fig. 7. Fourier-transform infrared spectroscopy (a) and X-ray diffraction (b) analysis of MgBC after adsorption.

contain $CdCO_3$, $Cd_3(PO_4)_2$ and $Cd(OH)_2$ [20,27]. It had been shown that the carbonate and phosphate contained in the biochar were released into the aqueous solution and thus reacted with $Cd^{2+}$/$Pb^{2+}$ in a precipitation reaction [16,26]. Furthermore, no characteristic peak of $Mg(OH)_2$ was detected in MgBC+Cd/Pb after adsorption, presumably because of the ion exchange of Mg with Cd/Pb [20,21,34].

In the overall spectrum, the characteristic peak of Mg 1s was detected in MgBC. Then, Mg 1s disappeared after adsorption. After Cd(II) and Pb(II) adsorption, the content of C–O decreased from 55.81% to 47.83% and 37.32%, respectively. Additionally, the proportion of C=O increased from 22.14% to 52.17% and 62.68%, respectively. This changes indicated that the complexation of O-functional groups participated in the adsorption [19,36]. Before adsorption, the content of Mg–O was 22.05%, but no Mg–O was detected after adsorption. This was consistent with the result that no obvious Mg 1s peak was observed in the adsorbed MgBC+Cd/Pb, which indicated that MgBC released Mg through ion exchange [7,20]. The X-ray photoelectron spectra after adsorption showed the characteristic peaks of Pb 4f and Cd 3d (Fig. 8a), indicating that Pb(II) and Cd(II) were successfully loaded on MgBC. The main forms of Pb(II) and Cd(II) adsorbed on MgBC can be $Pb^{2+}$/$Cd^{2+}$ and Pb–O/Cd–O [19,20]. The proportion of MgBC+Pb was 62.55% and 37.45%, respectively. The proportion of MgBC+Cd was 77.46% and 22.54%, respectively. Electrostatic interaction and ion exchange may lead to the binding of $Pb^{2+}$and $Cd^{2+}$ [1,17]. The Pb–O/Cd–O bond may be due to the complexation and precipitation of functional groups [2,36]. After adsorption, a series of Pb(II) and Cd(II) precipitates (e.g., lead carbonate, lead phosphate, $CdCO_3$ and $Cd_3SiO_5$) were observed in XRD [19,20]. Therefore, the complexation with O-containing functional groups and precipitation may be the reason for the adsorption of Pb(II) and Cd(II) on MgBC.

### 3.4. Adsorption–desorption experiments

After 8 adsorption–desorption experiments, the removal efficiency of Cd(II) and Pb(II) by MgBC decreased from 91.02% and 94.30% to 42.03% and 51.94%, respectively. Notably, the removal efficiency of both Cd(II) and Pb(II) by MgBC remained above 80% in the adsorption–desorption experiment for 4 times. This result was due to the loss of MgBC and the reduction of active sites. The above experiment shown that MgBC had the potential to be better applied for the removal of Pb(II) and Cd(II) from aqueous solution. Moreover, the concentration of $Mg^{2+}$ in the desorbed solution (Fig. 9b) and adsorbed solution (Fig. 9c) was also measured. After the first desorption, the concentration of $Mg^{2+}$ in the Cd(II) desorption solution and Pb(II) desorption solution was 1.14 and 1.23 mg/L, respectively, which

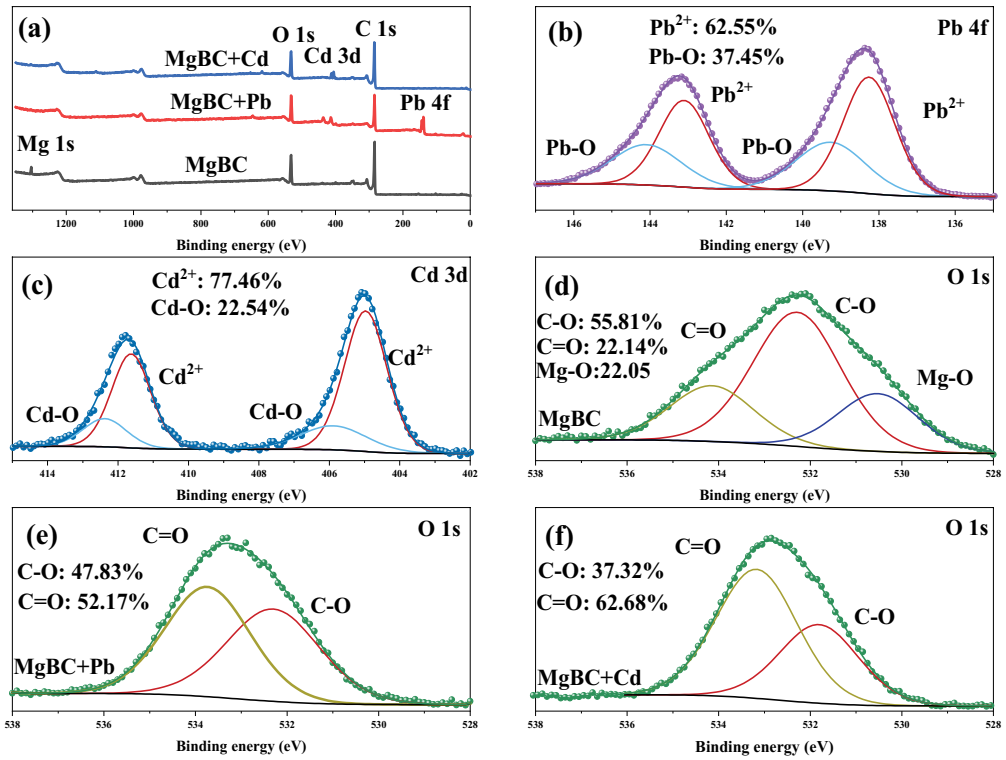


Fig. 8. X-ray photoelectron spectra of overall (a), Pb 4f (b), Cd 3d (c) and O 1s (d–f) before and after adsorption.

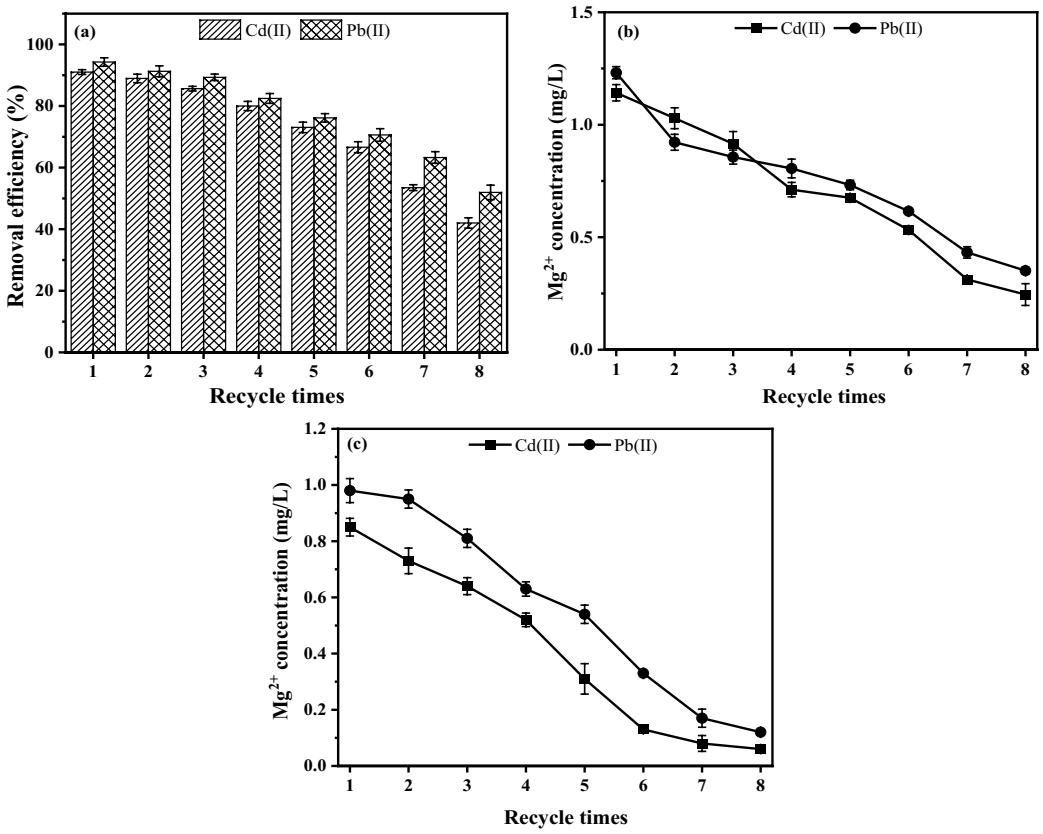


Fig. 9. Adsorption–desorption experiments of MgBC ($T$ = 25°C, dosage = 0.4 g/L, contact time = 300 min, pH = 6.0, $C_0$ = 10 mg/L and ratio 1:2). The concentration of $Mg^{2+}$ in the desorbed solution (b) and adsorbed solution (c).

presumably meaned that the HCl used as desorption agent dissolved the $Mg^{2+}$ on the MgBC. As desorption proceeded, the concentration of $Mg^{2+}$ in the desorbed solution gradually decreased. However, the solubility of $Mg^{2+}$ decreased in the adsorption solution and gradually decreased as the adsorption proceeded. Although, the $Mg^{2+}$ in MgBC gradually dissolved, and the removal efficiency of Cd(II) and Pb(II) after 4 adsorption–desorption experiments remained above 80%. This indicated that the Mg-modified rice straw biochar was a kind of potential adsorbent for Cd(II) and Pb(II).

## 4. Conclusion

The successful preparation of MgBC composites was confirmed by SEM, FTIR and XRD, with a reduction in specific surface area, pore volume and pore size, and successful loading of Mg on the surface. The adsorption processes of MgBC on Pb(II) and Cd(II) were in accordance with the pseudo-second-order kinetic model and Langmuir isotherm model, indicating that the adsorption was a homogeneous, monolayer chemisorption. The maximum adsorption capacities of MgBC on Cd(II) and Pb(II) were 73.77 and 119.52 mg/g, respectively. The removal mechanism included complexation, ions exchange, electrostatic interaction and co-precipitation. After 4 adsorption–desorption experiments, the removal efficiency of Cd(II) and Pb(II) by MgBC remained above 80%. The results shown that MgBC composites were effective in removing Cd(II) and Pb(II)-containing wastewater.

## Funding

This work was supported by National Natural Science Foundation of China (5167081086).

## Conflicts of interest

The author declare that we have no competing financial interests.

## References

[1] Y. Li, Y.Y. Liu, C.Y. Liu, L. Feng, S. Yang, Y.X. Shan, F. Xiao, Quantitatively ion-exchange between Mg(II) and Pb(II)/Cd(II) during the highly efficient adsorption by MgO-loaded lotus stem biochar, J. Taiwan Inst. Chem. Eng., 144 (2023) 104736, doi: 10.1016/j.jtice.2023.104736.

[2] A.Y. Li, W.Z. Ge, L.H. Liu, Y.T. Zhang, G.H. Qiu, Synthesis and application of amine-functionalized $MgFe_2O_4$-biochar for the adsorption and immobilization of Cd(II) and Pb(II), Chem. Eng. J., 439 (2022) 135785, doi: 10.1016/j.cej.2022.135785.

[3] W.B. Yu, J.W. Hu, Y.C. Yu, D.D. Ma, W.T. Gong, H.X. Qiu, Z.J. Hu, H.-W. Gao, Facile preparation of sulfonated biochar for highly efficient removal of toxic Pb(II) and Cd(II) from wastewater, Sci. Total Environ., 750 (2021) 141545, doi: 10.1016/j.scitotenv.2020.141545.

[4] Z. Ahmad, B. Gao, A. Mosa, H. Yu, X. Yin, A. Bashir, H. Ghoveisi, S. Wang, Removal of Cu(II), Cd(II) and Pb(II) ions from aqueous solutions by biochars derived from potassium-rich biomass, J. Cleaner Prod., 180 (2018) 437–449.

[5] Ç. Özer, M. İmamoğlu, Isolation of nickel(II) and lead(II) from aqueous solution by sulfuric acid prepared pumpkin peel biochar, Anal. Lett., 56 (2022) 491–503.

[6] C. Sun, T. Chen, Q. Huang, J. Wang, S. Lu, J. Yan, Enhanced adsorption for Pb(II) and Cd(II) of magnetic rice husk biochar by $KMnO_4$ modification, Environ. Sci. Pollut. Res. Int., 26 (2019) 8902–8913.

[7] Y.H. Tan, X.R. Wan, X. Ni, L. Wang, T. Zhou, H.M. Sun, N. Wang, X.Y. Yin, Efficient removal of Cd(II) from aqueous solution by chitosan modified kiwi branch biochar, Chemosphere, 289 (2021) 133251, doi: 10.1016/j.chemosphere.2021.133251.

[8] S. Usanmaz, C. Özer, M. Imamoglu, Removal of Cu(II), Ni(II) and Co(II) ions from aqueous solutions by hazelnut husks carbon activated with phosphoric acid, Desal. Water Treat., 227 (2021) 300–308.

[9] J. Xiao, R. Hu, G. Chen, Micro-nano-engineered nitrogenous bone biochar developed with a ball-milling technique for high-efficiency removal of aquatic Cd(II), Cu(II) and Pb(II), J. Hazard. Mater., 387 (2020) 121980, doi: 10.1016/j.jhazmat.2019.121980.

[10] R. Köklü, M. İmamoğlu, Removal of ciprofloxacin from aqueous solution by activated carbon prepared from orange peel using zinc chloride, Membr. Water Treat., 13 (2022) 129–137.

[11] D. Bal, Ç. Özer, M. İmamoğlu, Green and ecofriendly biochar preparation from pumpkin peel and its usage as an adsorbent for methylene blue removal from aqueous solutions, Water Air Soil Pollut., 232 (2021) 457–473.

[12] D.T. Tran, T.D. Pham, V.C. Dang, T.D. Pham, M.V. Nguyen, N.M. Dang, M.N. Ha, V.N. Nguyen, L.D. Nghiem, A facile technique to prepare MgO-biochar nanocomposites for cationic and anionic nutrient removal, J. Water Process Eng., 47 (2022) 102702, doi: 10.1016/j.jwpe.2022.102702.

[13] J. Xiang, Q. Lin, X. Yao, G. Yin, Removal of Cd from aqueous solution by chitosan coated MgO-biochar and its in-situ remediation of Cd-contaminated soil, Environ. Res., 195 (2021) 110650, doi: 10.1016/j.envres.2020.110650.

[14] H. Prasad Reddy Kannapu, S. Pyo, S. Shiung Lam, J. Jae, G. Hoon Rhee, M. Ali Khan, B.-H. Jeon, Y.-K. Park, MgO-modified activated biochar for biojet fuels from pyrolysis of sawdust on a simple tandem micro-pyrolyzer, Bioresour. Technol., 359 (2022) 127500, doi: 10.1016/j.biortech.2022.127500.

[15] Y. Xu, H. Tang, P. Wu, M. Chen, Z. Shang, J. Wu, N. Zhu, Manganese-doped hydroxyapatite as an effective adsorbent for the removal of Pb(II) and Cd(II), Chemosphere, 321 (2023) 138123, doi: 10.1016/j.chemosphere.2023.138123.

[16] D. Yang, L. Wang, Z.T. Li, X.J. Tang, M.J. He, S.Y. Yang, X.M. Liu, J.M. Xu, Simultaneous adsorption of Cd(II) and As(III) by a novel biochar-supported nanoscale zero-valent iron in aqueous systems, Sci. Total Environ., 708 (2020) 134823, doi: 10.1016/j.scitotenv.2019.134823.

[17] X.Q. Liu, D.D. Li, J.G. Li, J.L. Wang, S.J. Liang, H. Deng, A novel MnOx-impregnated on peanut shells derived biochar for high adsorption performance of Pb(II) and Cd(II): behavior and mechanism, Surf. Interfaces, 34 (2022) 102323, doi: 10.1016/j.surfin.2022.102323.

[18] M. Zahedifar, N. Seyedi, S. Shafiei, M. Basij, Surface-modified magnetic biochar: highly efficient adsorbents for removal of Pb(II) and Cd(II), Mater. Chem. Phys., 271 (2021) 124860, doi: 10.1016/j.matchemphys.2021.124860.

[19] F. Yang, Y.C. Chen, H.Y. Nan, L. Pei, Y.D. Huang, X.D. Cao, X.Y. Xu, L. Zhao, Metal chloride-loaded biochar for phosphorus recovery: noteworthy roles of inherent minerals in precursor, Chemosphere, 266 (2021) 128991, doi: 10.1016/j.chemosphere.2020.128991.

[20] J.W. Wu, T. Wang, J.W. Wang, Y.S. Zhang, W.P. Pan, A novel modified method for the efficient removal of Pb and Cd from wastewater by biochar: enhanced the ion exchange and precipitation capacity, Sci. Total Environ., 754 (2021) 142150, doi: 10.1016/j.scitotenv.2020.142150.

[21] A. Herath, C.A. Layne, F. Perez, E.B. Hassan, C.U. Pittman Jr., T.E. Mlsna, KOH-activated high surface area Douglas Fir biochar for adsorbing aqueous Cr(VI), Pb(II) and Cd(II), Chemosphere, 269 (2021) 128409, doi: 10.1016/j.chemosphere.2020.128409.

[22] B. Cao, J.H. Qu, Y.H. Yuan, W.H. Zhang, X.M. Miao, X.R. Zhang, Y. Xu, T.Y. Han, H.J. Song, S.Y. Ma, X. Tian, Y. Zhang, Efficient scavenging of aqueous Pb(II)/Cd(II) by sulfide-iron decorated biochar: performance, mechanisms and reusability exploration, J. Environ. Chem. Eng., 10 (2022) 107531, doi: 10.1016/j.jece.2022.107531.

[23] A. Li, W. Ge, L. Liu, G. Qiu, Preparation, adsorption performance and mechanism of MgO-loaded biochar in wastewater treatment: a review, Environ. Res., 212 (2022) 113341, doi: 10.1016/j.envres.2022.113341.
[24] D. Chen, Y. Yin, Y. Xu, C. Liu, Adsorptive recycle of phosphate by MgO-biochar from wastewater: adsorbent fabrication, adsorption site energy analysis and long-term column experiments, J. Water Process Eng., 51 (2023) 103445, doi: 10.1016/j.jwpe.2022.103445.
[25] S. Zhang, J. Wang, S. Zhu, X. Liu, Y. Xiong, H. Zhang, Effects of $MgCl_2$ and $Mg(NO_3)_2$ loading on catalytic pyrolysis of sawdust for bio-oil and MgO-impregnated biochar production, J. Anal. Appl. Pyrolysis, 152 (2020) 104962, doi: 10.1016/j.jaap.2020.104962.
[26] B. Zhao, T. Peng, R. Hou, Y. Huang, W. Zong, Y. Jin, D. O'Connor, S.K. Sahu, H. Zhang, Manganese stabilization in mine tailings by MgO-loaded rice husk biochar: performance and mechanisms, Chemosphere, 308 (2022) 136292, doi: 10.1016/j.chemosphere.2022.136292.
[27] S. Cheng, S. Zhao, H. Guo, B. Xing, Y. Liu, C. Zhang, M. Ma, High-efficiency removal of lead/cadmium from wastewater by MgO modified biochar derived from crofton weed, Bioresour. Technol., 343 (2022) 126081, doi: 10.1016/j.biortech.2021.126081.
[28] Z. Feng, N. Chen, T. Liu, C. Feng, $KHCO_3$ activated biochar supporting MgO for Pb(II) and Cd(II) adsorption from water: experimental study and DFT calculation analysis, J. Hazard. Mater., 426 (2022) 128059, doi: 10.1016/j.jhazmat.2021.128059.
[29] J.X. Xiang, Q.T. Lin, X.S. Yao, G.C. Yin, Removal of Cd from aqueous solution by chitosan coated MgO-biochar and its *in-situ* remediation of Cd-contaminated soil, Environ. Res., 195 (2021) 110650, doi: 10.1016/j.envres.2020.110650.
[30] X. Meng, R. Hu, Nitrogen/phosphorus enriched biochar with enhanced porosity activated by guanidine phosphate for efficient passivation of Pb(II), Cu(II) and Cd(II), J. Mol. Liq., 323 (2021) 115071, doi: 10.1016/j.molliq.2020.115071.
[31] T. Cai, H. Du, X. Liu, B. Tie, Z. Zeng, Insights into the removal of Cd and Pb from aqueous solutions by NaOH–EtOH-modified biochar, Environ. Technol. Innovation, 24 (2021) 102031, doi: 10.1016/j.eti.2021.102031.
[32] C. Hong, Z. Dong, J. Zhang, L. Zhu, L. Che, F. Mao, Y. Qiu, Effectiveness and mechanism for the simultaneous adsorption of Pb(II), Cd(II) and As(III) by animal-derived biochar/ferrihydrite composite, Chemosphere, 293 (2022) 133583, doi: 10.1016/j.chemosphere.2022.133583.
[33] Y. Cao, S. Jiang, Y. Zhang, J. Xu, L. Qiu, L. Wang, Investigation into adsorption characteristics and mechanism of atrazine on nano-MgO modified fallen leaf biochar, J. Environ. Chem. Eng., 9 (2021) 105727, doi: 10.1016/j.jece.2021.105727.
[34] G.H. Mo, J. Xiao, X. Gao, To enhance the $Cd^{2+}$ adsorption capacity on coconut shell-derived biochar by chitosan modifying: performance and mechanism, Biomass Convers. Biorefin., (2022), doi: 10.1007/s13399-021-02155-9.
[35] J.W. Wu, T. Wang, Y.S. Zhang, W.P. Pan, The distribution of Pb(II)/Cd(II) adsorption mechanisms on biochars from aqueous solution: considering the increased oxygen functional groups by HCl treatment, Bioresour. Technol., 291 (2019) 121859, doi: 10.1016/j.biortech.2019.121859.
[36] S.H. Cui, R. Zhang, Y.T. Peng, G. Xing, Z. Li, B.B. Fan, C.Y. Guan, J.Z. Beiyuan, Y.Y. Zhou, J. Liu, Q. Chen, J. Sheng, L.L. Guo, New insights into ball milling effects on MgAl-LDHs exfoliation on biochar support: a case study for cadmium adsorption, J. Hazard. Mater., 416 (2021) 126258, doi: 10.1016/j.jhazmat.2021.126258.